Title
PROGRESS IN SORPTION SEPARATIONS: ADSORPTION, DIALYSIS. AND ION EXCHANGE

Author
Vermeulen, Theodore.

Publication Date
1959-04-07

UCRL-8718

UNIVERSITY OF CALIFORNIA

Radiation Laboratory

BERKELEY, CALIFORNIA

DISCLAIMER

UCRL-8718

UNIVERSITY OF CALIFORNIA
Lawrence Radiation Laboratory
Berkeley, California

Contract No. W-7405-eng-48

PROGRESS IN SORPTION SEPARATIONS: ADSORPTION, DIALYSIS, AND ION EXCHANGE

Theodore Vermeulen

April 7, 1959

Printed for the U. S. Atomic Energy Commission

UCRL-8718

PROGRESS IN SORPTION SEPARATIONS: ADSORPTION, DIALYSIS, AND ION EXCHANGE

Theodore Vermeulen

Lawrence Radiation Laboratory and Department of Chemical Engineering
University of California, Berkeley, California

April 7, 1959

ABSTRACT

Calculation methods for fixed-bed and countercurrent column separations are reviewed. The controlling factors in performance are shown to be the equilibrium isotherm and the effective rate of mass transfer (which may include longitudinal dispersion). A general correlation of experimental rate data is given, and comparison is made between theory and experiment in a few representative cases. Finally, moving-bed and fixed-bed columns are compared to determine the conditions under which their behavior is identical.

PROGRESS IN SORPTION SEPARATIONS: ADSORPTION, DIALYSIS, AND ION EXCHANGE

A. DESIGN PRINCIPLES FOR GRANULAR-MATERIAL OPERATIONS*

T. Vermeulen

The appropriate design method to be followed depends mainly on the process arrangement selected -- that is, upon whether the separation is to be carried out in batch (staged) equipment, or semi-continuous (fixed-bed), or continuous (countercurrent) equipment. Once the calculation method is determined, the most general factor in design is the stoichiometry of the separating agent. In the case of adsorption or dialysis, the stoichiometry will be determined by the equilibrium behavior between the fluid and solid phases; for a given ion-exchange material, the sorption capacity is usually independent of the exchanging ion-pair and its particular equilibrium.

With well-known operations such as water softening, practical design often involves only the sorption capacity and an empirical efficiency factor. In less routine separations, a more accurate prediction of performance should be made. Here equilibrium data are essential, along with actual rate values or values estimated from general mass-transfer theory. A complete design will require the use of at least three dimensionless variables, which correspond to a stoichiometric throughput ratio (Z), an equilibrium parameter (r), and a number of transfer units (N). In turn, N depends upon

---

*Part of the work reported here was done in the E. O. Lawrence Radiation Laboratory, under the auspices of the U.S. Atomic Energy Commission.

the molecular-diffusion Péclet number (to be defined), upon the distribution ratio between phases (D), and upon what mass-transfer mechanism is rate controlling.

1. Equilibrium Relationships

In systems with only two fluid-phase components, a solvent and one solute, a simple plot can be drawn of the solute concentration in the solid phase, as a function of its concentration (or partial pressure) in the fluid phase. Each such curve holds at only one particular temperature, and hence is known as an "isotherm."

Three types of equilibrium are shown schematically in Figure 1, with the solid-phase concentration as ordinate and the fluid-phase concentration as abscissa. Different types of column behavior will be obtained, depending upon the curvature of the isotherm. If the plot is concave upward, adsorption is less favorable at low concentrations than at higher ones, and the equilibrium is classed as "unfavorable." If the plot is convex upward, regardless of its absolute value, the adsorption is "favorable." A simple "linear" curve is intermediate; and many dialysis equilibria are linear or nearly so. More complex isotherms are possible which are made up of both unfavorable and favorable portions.

Isotherms can also be expressed in terms of relative fluid- and solid-concentrations (x and y respectively), based on the maximum concentration levels encountered in a particular separation; here $x = c/C_o$ or p/p_o and $y = q/q_o^*$, where C_o or p_o is feed concentration or partial-pressure, and q_o^* is the solid concentration in equilibrium with it. This type of plot is shown in Figure 2; in such a diagram, used first for ion exchange, the reason for the terms "unfavorable"

and "favorable" becomes more evident.

The design of fixed-bed separations centers about the calculation of breakthrough curves, and wherever possible this is done in terms of algebraic equations. Because the equilibrium determines the type of breakthrough equation to use, efforts are made to represent the isotherm by equations which fulfill the following limitations: Either the isotherm relation itself (for favorable equilibria) or its derivative (for unfavorable equilibria) must be in a form that is explicit in the fluid-phase concentration. For gas-phase adsorption, the equation proposed by Sips (34) and extended by Koble and Corrigan (26) is one that meets these conditions, and combines the properties of the well-known Langmuir and Freundlich isotherms.

$$q = \frac{aK_C p^M}{1 + K_C p^M} \tag{1}$$

where p is the partial pressure of solute; and a, K_C, and M are adjustable constants. If $a = q_m$, the extent of adsorption in a monomolecular layer, this transforms to

$$\frac{q}{q_m} = \frac{K_C p^M}{1 + K_C p^M} \tag{2}$$

To fit a "relative" isotherm, Equation (2) is rewritten for q_o^* in terms of p_o. Dividing this new relation into Equation (2), and setting $x = p/p_o$, gives

$$y = \frac{q}{q_o^*} = \frac{(1 + K_C')x^M}{1 + K_C' x^M} \tag{3}$$

where $K_C' = K_C p_o^M$. This result can also be obtained directly from Equation (3), by a different choice of a; that is, $a = q_o^* (1 + K_C p_o^M)/K_C p_o^M$. Unlike the preceding expressions, Equation (3) also fits adsorption from a liquid phase. If $M < 1$ and also $M < (1 + K_C')/(1 - K_C')$, Equation (2) will represent an equilibrium that is favorable throughout its range; or, if M is greater than each of these criteria, an equilibrium that is unfavorable throughout.

A guide to ion-exchange equilibria is given by the Donnan membrane-equilibrium relation (10). As observed by Bauman and Eichhorn (4) and developed theoretically by others (18,33), there is a small uptake of free electrolyte into a resin, with equivalent concentrations $c^R_{M^{m+}} = c^R_{X^{n-}}$, which provides an appreciable concentration of oppositely charged ion. The equilibrium then provides that the activity product (relative to a single standard state) must be equal in the solution and in the resin phase:

$$(c_{M^{m+}})^n (c_{X^{n-}})^m \gamma_{MX} = (q_{M^{m+}} + c^R_{M^{m+}})^n \nu^n_{M^{m+}} (c^R_{X^{n-}} \nu_{X^{n-}})^m \qquad (4)$$

where γ and ν are solution and resin-phase activity coefficients, respectively. A second cation M_2, exchanging with the first M_1, will conform to a similar relation. The first of these expressions may be divided by the second, to eliminate the anion concentrations; with c^R neglected relative to q, the quotient equation reduces to the mass-action expression:

$$\frac{(c_{M_2})^{m_1}\,(q_{M_1})^{m_2}}{(c_{M_1})^{m_2}\,(q_{M_2})^{m_1}} = \frac{(\nu_{M_2})^{m_1}\,\gamma_{(M_1)X}^{\,m_2/n}}{(\nu_{M_1})^{m_2}\,\gamma_{(M_2)X}^{\,m_1/n}} = K \qquad (5)$$

As Rice and Harris (33) have shown, the Donnan equilibrium indicates a larger uptake of anion by the resin when it contains more of a higher-valence cation; thus the activity coefficients for the resin phase, in particular, will not remain constant as exchange progresses, and K will not approach a true constant except in the homovalent case ($m_1 = m_2$). Empirically the effect of such factors is to fit a mass-action expression with the exponent ratio m_2/m_1 part way between unity and its true value. In general, Equation (4) is not explicitly soluble for c_{M_1} in the ways needed for breakthrough calculation, and recourse must be had to Equation (1).

As a practical matter, the true isotherm will usually be fitted approximately (whatever the valences involved) with a homovalent type of mass-action equation. For a binary equilibrium involving pure resin B and pure solution A at the start (23),

$$\frac{q_A\,(C_o - c_A)}{c_A\,(Q - q_A)} = (K^{II})_{AB} = \frac{1}{r_{AB}} \qquad (6)$$

where r is the equilibrium parameter or separation factor, analogous to the relative volatility in distillation calculations; and Q is the total equivalent concentration of all ions in the resin phase. This relation is convenient to use and gives sufficient accuracy in most cases, even when $m_1 \neq m_2$.

The type of fit which may be obtained in a relatively extreme case is shown in Figure 3 for the data of Vasishth and David (40) on the exchange reaction

$$Fe^{+++} + 3HR \rightleftharpoons FeR_3 + 3H^+$$

where R represents Dowex 50 resin, and the anion present is ClO_4^-. The solid curve corresponds to Equation (5), with $M_1 = Fe$, $M_2 = H$, $m_1 = 3$, and $m_2 = 1$. The value of $(K^{II})_{Fe/H}$ determined from Equation (6) will range from 52.3 to 3.74. However, a satisfactory average is given by the point where $y = 1 - x$; namely, $K^{II} = 8.0$.

For binary ion exchange involving resin that initially contains a uniform mixture of ions A and B, and a feed solution also comprising A and B, the solution concentration will range between x_o^* and x_o as the relative concentration (now, λ) increases from zero to unity; likewise, for the resin phase, the relative concentration $\omega = 0$ corresponds to $y_A = y_o$, and $\omega = 1$ corresponds to $y_A = y_o^*$. The equilibrium parameter (45) then becomes

$$r = \frac{\lambda(1 - \omega)}{\omega(1 - \lambda)} = \frac{(K^{II} - 1)x_o^* + 1}{(K^{II} - 1)x_o + 1} \qquad (7)$$

For adsorption in a column initially solute free, the same separation factor r can be defined for the "relative" isotherm, Equation (3), but only with $M = 1$. Then,

$$r = \frac{x(1 - y)}{y(1 - x)} = \frac{1}{1 + K_o p_o} \qquad (8)$$

2. Kinetics

The effective rate of exchange or adsorption is determined by one or more of several alternate diffusional steps, as follows:

1. Mass transfer from the flowing phase to the external surfaces of the sorbent particles.

2. Pore diffusion in the fluid phase, within the particles (for most adsorbents, inorganic zeolites, and certain newly developed ion-exchange resins).

3. Reaction at the phase boundaries (usually immeasurably fast).

4. Diffusion in the solid phase (or, for an adsorbent, diffusion in the adsorbed surface layer).

5. In cases of moderately high mass transfer with extremely slow flow rates, the breakthrough curves may be broadened by either eddy dispersion or molecular diffusion in the longitudinal direction.

The various modes of mass transfer are often handled in an apparent-reaction-rate treatment, for mathematical simplicity. The driving-potential expression, when combined with one of the equilibrium-parameter relations (Equations 6-8), is converted into a reaction-kinetic form exhibiting second-order behavior in both the forward and the reverse directions:

$$\frac{dy}{d\tau} = \frac{Kb}{\underset{\sim}{D}}[x(1 - y) - ry(1 - x)] \qquad (9)$$

where τ is time; $\underset{\sim}{D}$ is the distribution ratio of solute between solid and fluid ($q_o^* \rho_b / C_b \epsilon$), with ρ_b the bulk density of the

packing, and ϵ the void fraction in the column exterior to the particles; and b is a correction factor which is often near unity (22), and nearly constant except for highly favorable equilibria ($r \sim 0$). (When r is small, more exact rate equations are used which do not introduce b, and a different approximation is introduced to render such expressions integrable.) The conductance term, K, is the product of the effective mass-transfer coefficient and an interfacial area per unit volume, and has dimensions of reciprocal time.

3. Fixed-Bed Performance

Performance studies for fixed-bed columns are concerned with the concentration history of the column effluent -- that is, with the variation in concentration as a function of time or of volume of effluent. Concentration calaulations must make use of one or another of a group of specialized results which take the place of a general solution to the problem. The specialized results can be identified on the basis of controlling mechanism (from among those listed above) and of equilibrium behavior (unfavorable, linear, favorable, or completely irreversible).

Often it is a major problem to locate the particular case that applies to a specific situation. Because of the variety of possible mechanisms, rates determined experimentally cannot safely be extrapolated to other operating conditions except with full knowledge of the theoretical behavior. A trial classification of the various special cases in column-performance theory, in terms of the equilibrium and rate conditions involved, has been given

in a recent review paper (43).

To achieve a reasonable generality in the mathematical analysis, dimensionless groups must be formed from the numerous variables, as has already been indicated. Among these groups is the number of transfer units, N, or the number of apparent reaction units, N_R, defined as follows:

$$N = \frac{N_R}{b} = \frac{Kh}{U} \qquad (10)$$

where h is the column height, and U is the linear flow rate through the column (superficial velocity divided by porosity). The N.T.U. and N.R.U. have been called "column-capacity parameters" (Σ and s respectively) in earlier work by one of the present authors (22,23); and "thickness modulus" by Hougen and Marshall (24).

The H.T.U. ($H = h/N$) is generally a function of the Reynolds and Schmidt groups. Empirically, these two groups enter to nearly the same power; hence their product, the Péclet group for mass transfer, can be used:

$$N_{Pe} = \frac{d_p U \epsilon}{6(1-\epsilon)D_f} \qquad (11)$$

where D_f is the molecular-diffusion coefficient for the fluid phase. The H.T.U. is made dimensionless by dividing it into particle diameter to give the Colburn group ($N_{Co} = d_p/H$).

Use has been made of a large body of published breakthrough data, to arrive at correlations which isolate the separate effects of external and internal diffusion and indicate the experimental onset of eddy dispersion at low flow rates (22, 46). One such

correlation is shown in Figure 4.

Addition of resistances, i.e. of reciprocals of the conductances, can be carried out with the aid of the b factors (22, 43) to give the effective over-all rate coefficient K for Equation (9):

$$\frac{1}{Kb} = \frac{1}{K_f b_f} + \frac{1}{K_{pore} b_f} + \frac{1}{K_p b_p} + \frac{1}{K_L b} \qquad (12)$$

Here, subscript f designates the fluid phase, p the particle phase, and L the contributions of longitudinal eddy dispersion and/or molecular diffusion. This method of combining various mass-transfer resistances has long been known (cf. 14, 34); and in recent years their additivity with the longitudinal-dispersion effects has been established by Lapidus and Amundson (25) and Van Deemter and co-workers (38).

The mass-transfer coefficient for external diffusion, with spherical particles having $\epsilon = 0.4$, provides the following value for the coefficient K_f:

$$K_f = \frac{6.3}{d_p}\left(\frac{D_f U \epsilon}{d_p}\right)^{0.5} \qquad (13)$$

The coefficient for solid-phase internal diffusion is a direct function of the particle-phase diffusivity:

$$K_p = \frac{60\, D_p}{\underset{\sim}{D}\, d_p^2} \qquad (14)$$

For ion exchange, in particular, Boyd and co-workers (7,8) have reported extensive basic data on resin-phase diffusivities.

A similar equation applies for fluid-phase pore diffusion within the solid structure:

$$K_{pore} = \frac{60\, D_{pore}}{d_p^2} \qquad (15)$$

with the diffusivity D_{pore} always less than D_f for the corresponding bulk fluid.

The apparent conductance for longitudinal dispersion, channeling, and molecular-diffusion effects is

$$K_L = U^2/E = U/L \qquad (16)$$

where E is the dispersion coefficient or diffusivity that describes this process; and L is an effective mixing length. Experimental studies yield

$$L = \frac{d_p \epsilon}{[(N_{Pe})_\ell \epsilon](Q + 1)} \qquad (17)$$

The Péclet-group term for dispersion, $(N_{Pe})_\ell \epsilon$, is approximately 1/6 for liquids in laminar flow (9, 13, 25); and about 2/3 for liquids in turbulent flow (25) or for gases in either flow regime (30).

Experimental data for H.T.U. can be compared with Figure 4 in order to provide numerical values for the diffusivities D_f and D_p (with D_{pore} included implicitly in the latter). Once these two diffusivities are known, together with essential equilibrium and concentration data, Figure 4 is of general use for predicting the N -- and hence the breakthrough curve -- for any proposed operating condition.

In recording the concentration history for a column effluent, the independent variable is the total time of passage of solution, or the total volume of solution passed through the column, or some

function proportional to each of these two terms. A throughput ratio can be defined which expresses the total moles of solute fed, as a function of the stoichiometric capacity of the column:

$$Z = \frac{V - hS\epsilon}{V_{stoic}} = \frac{V - hS\epsilon}{\underset{\sim}{D}hS} \qquad (18)$$

Here V is the volume of feed solution introduced, hS is the void-volume of the column, and V_{stoic} is the volume of feed which would just saturate the column if exchange were complete. The product NZ or $N_R Z$ is used frequently; it has been called a "solution-capacity parameter" or a "time modulus" and is also designated by ⓗ or t.

The relative steepness (or "sharpness") of breakthrough curves increases with decreasing r, and with increasing N. Typical behavior is indicated in Figure 5, for a combination of three values of r and three values of N. The curves for r = 0.5 correspond to a favorable equilibrium, and exhibit a "constant-exchange-zone" shape or "constant pattern". Such curves are termed "self-sharpening" because their slope increases if the abscissa is expressed on a stoichiometric basis; i.e., on a Z scale. Experimental data illustrating this case will be given below. The essential derivations have been published by Drew, Spooner, and Douglas (12) and Michaels (31) for external diffusion controlling; by Wicke (48), Glueckauf and Coates (17), and Vermeulen (42) for internal diffusion; by Acrivos (1) for pore diffusion; and by Bohart and Adams (5) and Sillén (35) for the reaction-kinetic method.

The other extreme of behavior is shown by the curves for r

= 2 (an unfavorable equilibrium) which follow a "proportionate pattern." Relative to the stoichiometric breakthrough point, these curves show no tendency to increase in sharpness. This case has been treated by DeVault (10), Walter (46), Wilson (49), and Weiss (47).

The behavior of the linear-equilibrium curves (r = 1) is seen to fall between the other two limiting cases. The available solution for the analogous case of regenerative heat transfer was first applied to ion exchange and adsorption by Beaton and Furnas (5), Boyd, Myers, and Adamson (7), and Hougen and Marshall (24).

Breakthrough equations are obtained by solving a rate expression simultaneously with the material-balance (or "continuity") relation,

$$\left(\frac{\partial y}{\partial ZN}\right)_N = -\left(\frac{\partial x}{\partial N}\right)_{ZN} \tag{19}$$

For the general case of a non-linear equilibrium, the rate is given by Equation (9) which can be rewritten in dimensionless terms:

$$\left(\frac{\partial Y}{\partial ZN}\right)_N = x(1 - y) - ry(1 - x) \tag{20}$$

At any one value of r, an entire family of breakthrough curves is needed to describe the solutions of Equation (22) for different values of N. Figure 6 shows such a family plotted for r = 1. This result, originally obtained by Anzelius (2) for heat transfer, is useful in solving analytically for non-linear equilibria ($r \neq 1$) and is therefore designated as a special function J. By comparison

with Figure 5, it is seen that these curves would be S-shaped if they were plotted on linear coordinates.

The explicit solution of the general non-linear case was first obtained by H. C. Thomas (38). It can be expressed as

$$x = \frac{\underset{\sim}{J}(rN_R, ZN_R)}{\underset{\sim}{J}(rN_R, ZN_R) + e^{(r-1)N_R(Z-1)}\left[1 - \underset{\sim}{J}(N_R, rZN_R)\right]} \qquad (21)$$

Cross-plots and numerical tables for this solution have been computed by Hiester and coworkers (22,32). A rapid approximate method for breakthrough-curve estimation, applying to this situation as well as to the others considered above, has been given recently by Vermeulen and Hiester (43). For $r < 0.5$ and $r > 2$, Equation (21) generally reduces to simpler forms that represent the constant-pattern case and the proportionate-pattern case, respectively.

Constant-pattern behavior is shown in Figure 7 by two curves for ferric-ion breakthrough, from Dowex-50 beds initially in the hydrogen form, as reported by Vasishth and David (40). The left-hand curve corresponds to a shorter column (45.5 cm.) and higher concentration level (0.51 N); the right-hand curve is for a 61 cm. column, at 0.40 N. The principal rate-determining mechanism is solid-phase diffusion, as shown by the fit of the solid curves. The dashed curves, for external diffusion and for pore diffusion (which is certainly inapplicable) have entirely different shapes. The breakthrough equation applicable to solid-phase diffusion (42) is

$$(c/C_o)^2 = 1 - e^{-NZ + N - 0.614} \qquad (22)$$

In plotting these curves, it has been assumed that $r = 0$. The observed deviations in shape may be due partly to this assumption, partly to the presence of channeling and longitudinal dispersion, and partly to the range of particle sizes used (20-50 mesh, rather than a single uniform diameter).

4. Chromatography

In chromatography, only a small amount of feed solution, containing the components to be separated, is admitted to the column. These solute components are then carried through (eluted) by a carrier phase (the elutant) that initially is free of them. The solutes travel through the column as bands or zones at slightly different velocities. If the column is long enough, the zones will draw apart completely from one another, and may be recovered in the effluent as separate solutions of each individual solute.

The term "chromatography" stems from the fact that colored plant extracts were the first materials to be separated by this method. It now applies to any situation in which two or more mixed solutes are fed to a column, and are then eluted under conditions which provide at least a partial separation.

Movement of each zone through the adsorbent occurs by the following mechanism: Fluid on the upstream (trailing) side of a zone is undersaturated with respect to the adsorbed component and continually takes it into solution. Passing beyond the peak of the zone to the downstream (leading) side, the same fluid is supersaturated relative to coexisting adsorbent and hence gradually redeposits the solute component.

A zone obeying a linear equilibrium would retain a constant rectangular shape, in the event that complete equilibrium could be maintained between solution and resin at each point in the column at all times during its elution. Actually, equilibrium cannot be maintained, because of the mass-transfer resistances and also longitudinal dispersion, and hence the zone undergoes a continual spreading. An initially rectangular shape changes to a flattened-top bell shape, and this in turn develops into a fully peaked bell shape.

A linear equilibrium ($r = 1$) is approached in many cases. The equilibrium parameter given by Equation (7) is applicable to nearly all chromatographic separations, with $x_o^* = 0$. Thus, as x_o (the effective feed concentration of the solute in its mixture with carrier component) is decreased, r changes from its reference value of $1/K^{II}$ and becomes progressively nearer to unity. For "trace" chromatograms where r is within about 10% of unity, with $N_R > 50$ and $Z_{sat} < \sqrt{\pi/N_R}$, a Gaussian-distribution equation is obtained (15,23,44):

$$c_A/(c_A)_{max} = e^{-(N_R/4)(Z' + 0.5\, Z_{sat} - 1)^2} \qquad (23)$$

where Z' is measured from the start of the elution period. This same result is obtained from the "plate theory" (28,29), with the number of theoretical plates equal to one-half the N.T.U. or N.R.U.

A relative sharpening of each zone occurs as the length of column traversed increases, because the spreading of the zone is approximately proportional to the square root of the column length;

whereas the total volume of elutant required, for complete elution of the zone, is almost directly proportional to the column length. Thus, the longer the column (or, more specifically, the greater the N.T.U.), the more complete is the isolation of the separate solutes.

Asymmetric elution curves are common and can often be attributed to deviations of r from unity -- i.e., to non-"trace" conditions. With a favorable equilibrium for saturation ($r < 1$), the leading edge of the zone -- the first to emerge in the effluent -- will be steeper than the trailing edge; if $r > 1$ for saturation, the leading edge will be more sloping than the trailing edge. Representative zone shapes for $r < 1$, $r = 1$, and $r > 1$ are given in Figure 8, where concentration is the ordinate and effluent volume is the abscissa.

A typical non-Gaussian chromatogram, from data of Baddour and Hawthorn (3), is given in Figure 9. The solid curve shows the fit obtained with the exact equation (3,23), using a value of $r = 0.589$. The dashed curve is the Gaussian approximation, obtained from Equation (23), with the change that Z' and Z_{sat} are each multiplied by r.

It is seen that the overlap between consecutive chromatograms will not be predicted correctly by the Gaussian-equation treatment. However, the more detailed mass transfer theory has been used to select systematically the optimum values of elutant concentration, pressure drop through the column, flow rate, total cycle period, charge period, recycle feed rate, multiple cycling, concentration of complexing agent, and number of stages of operation, for

representative systems.

5. Countercurrent Separations

A connecting link between fixed-bed and moving-bed separations is provided by the constant-pattern case of fixed-bed operation which arises with favorable equilibria ($r \leq 0.5$). As Michaels (31) has shown, the breakthrough curve for this case can be derived by considering the adsorption wave or exchange zone as a stationary pattern, with the resin phase and the fluid phase in countercurrent motion at the requisite velocities. Almost without regard to the mechanism that is assumed, either a derivation by the usual mass-transfer methods for countercurrent operations or a simultaneous solution of Equations (19) and (20) for this case will yield an equation in the general form:

$$f(x) = NZ - N \tag{24}$$

to express the constant-pattern curve for effluent concentration from a fixed bed. For solid diffusion controlling at $r = 0$, for example, $f(x)$ from Equation (22) is $- \ln(1 - x^2) - 0.614$; for external diffusion at $r = 0$, $f(x) = 1 + \ln x$.

To solve Equation (24) for constant time, a new variable must be introduced: $(NZ)_o$, the dimensionless throughput volume (or time) measured at the column inlet. Then $(NZ)_N = (NZ)_o - (N/\underset{\sim}{D})$; and, at any single time,

$$f(x_2)_{(NZ)_o} - f(x_1)_{(NZ)_o} = \frac{\underset{\sim}{D} + 1}{\underset{\sim}{D}} (N_1 - N_2) \tag{25}$$

where subscripts 1 and 2 designate two different heights in the column.

A practical fixed-bed column always contains a height of sorbent that is substantially greater than the height of the exchange zone. Hence the solid at the point of feed entrance is used virtually to capacity; and stoichiometry determines the rate of movement of the adsorption wave relative to the solid. In the particular moving-bed case that is analogous to the fixed bed, the "extraction factor" $\underset{\sim}{E}$, defined as follows, is unity:

$$\underset{\sim}{E} = \underset{\sim}{D}\, F_p/F_f \tag{26}$$

where F_p and F_f are scalar volumetric flowrates of solid and fluid, respectively, measured relative to a stationary column-wall; and $F_p + F_f (= F)$ gives the flow of either phase relative to the other; also, $F_p = U_p S(1 - \epsilon)$ and $F_f = U_f S\epsilon$, where the U's are linear velocities and S is the superficial cross-sectional area of the column.

For a moving bed, the mass-transfer derivation at $\underset{\sim}{E} = 1$ with the fluid-phase resistance controlling serves as a model for any $\underset{\sim}{E}$ and any mechanism:

$$\frac{dq}{dt} = U_p\, \rho_p\, q_o^* \frac{dy}{dh} \tag{27}$$

or

$$\frac{dq}{dt} = - U_f\, C_o \frac{dx}{dh} = K_f\, C_o\, (x - x^*) \tag{28}$$

In general, x^* is known in terms of y; and y, through material balance, can be replaced by a function of x. In the present irreversible case, $x^* = 0$, and Equation (28) leads to the solution:

$$f(x) = 1 + \ln x = \text{const.} - N_F \tag{29}$$

where $N_F (= K_f h/U_f)$ is the N.T.U. for a moving bed, based upon the

fluid phase. By reference to Equation (10), with $U/U_f = (\underset{\sim}{D} + 1)/\underset{\sim}{D}$ when $\underset{\sim}{E} = 1$, the results of Equations (25) and (29) are seen to coincide.

As a more general relation, these considerations yield

$$N_F = N\ U/U_f \tag{30}$$

When N_P is large, N_F approaches the over-all number of fluid-phase transfer units N_{OF}. Likewise, when N_F is large, $N_P \longrightarrow N_{OP}$. The N_{OF} or N_{OP} for a given separation can be evaluated by either analytical or graphical methods, in the same way as for absorption or extraction.

For design purposes, the column height h for a given separation can be predicted from the product of the over-all N.T.U. and the corresponding H.T.U. (H_{OF} or H_{OP}). These in turn must be obtained from correlational values for the separate phases; under non-linear equilibria, at a constant r, these H.T.U.'s can be added in the following way:

$$H_{OF} = \frac{1}{b_f}\left[H_F + \frac{H_P}{\underset{\sim}{E}}\right] \tag{31}$$

Because of the lack of accurate rate data for moving-bed systems up to the present time, a stagewise graphical calculation of the number of equivalent theoretical contacts N_e will often be as useful as a more precise computation of N_{OF}. Figure 10, from work of Hiester and associates, illustrates a hypothetical separation of two trace ions A and B in the presence of a "gross" component, for a saturation section having two theoretical contacts. "The two ions are present in equimolar concentrations in the feed,

and the entering resin is free of A and B. The operating lines for the two ions are parallel. Because the slope of the equilibrium line for B is greater than for A, the concentration of the solution is reduced much further in B than in A. Thus the effluent solution is enriched in A, and the effluent resin is enriched in B" (21).

As pointed out by those authors, a simple relation exists between N_c and over-all N.T.U. in those cases where $\underset{\sim}{E}$ is constant:

$$N_{OF} = \underset{\sim}{E}\, N_{OP} = N_c\, \underset{\sim}{E}\, (\ln \underset{\sim}{E})/(\underset{\sim}{E} - 1) \qquad (32)$$

In a tapped-screen moving-bed contactor, apparent H.T.U.'s were measured by Hiester, Fields, Phillips, and Radding (21), which included large effects due to longitudinal dispersion; their results fit the relations

$$\frac{H_F D_p}{d_p^2 U_f} = \frac{15}{\epsilon^{1/2}} \frac{D_p}{D_f} \left(\frac{D_f}{U d_p}\right)^{1/2} \qquad (33)$$

and

$$\frac{H_p D_p}{d_p^2 U_p} = \frac{0.60}{\underset{\sim}{D}(1-\epsilon)} \qquad (34)$$

Further theoretical interpretation of these results can be expected in the future.

NOTATION

b correction factor for computing apparent kinetic rate from mass-transfer rates, or for combining mass-transfer resistances

c concentration of solute in the fluid phase

C_o total concentration of solutes in the fluid phase; or concentration of solute in the feed

$\underset{\sim}{D}$ distribution parameter, or ratio of concentrations in the particle and fluid phases

D diffusivity

d_p particle diameter

$\underset{\sim}{E}$ extraction factor; $\underset{\sim}{D}\, F_p/F_f$

F volumetric flow rate

f function

h column height

H H. T. U. (or H. R. U.)

$\underset{\sim}{J}$ column-saturation function

K equilibrium constant

m,n valences

N number of transfer units, or column-capacity parameter for mass transfer

N_e number of equilibrium contacts, Equation (32)

N_R number of reaction units, or column-capacity parameter for reaction-kinetic treatment

p partial pressure

q concentration of solute in the particle phase

Q ultimate exchange capacity of the particle phase

r equilibrium parameter

S cross-sectional area of column

s column-capacity parameter, for reaction-kinetic treatment; N_R

t solution-capacity parameter, for reaction-kinetic treatment; $N_R Z$

U actual mean linear flowrate of fluid phase relative to solid; U_f, U_p are flow rates relative to column wall

V volume of feed solution entering column

x dimensionless solution concentration; c/C_o

y dimensionless solid-phase concentration; q/q_o^*, or q/Q

Z throughput parameter, or ratio of actual volume of effluent to the stoichiometric volume

γ activity coefficient for solution phase

ϵ ratio of void space outside particles to total volume of column

ζ mechanism parameter; $Q K_p/K_f$, in Figure 4

$\ominus$ solution-capacity parameter, for mass-transfer treatment; NZ

K rate coefficient

λ extent of saturation of solution phase, with reference to initial and final concentrations

ν activity coefficient for resin phase

ρ_b bulk packed density of air-dried particles

Σ column-capacity parameter for mass-transfer treatment; N

τ time

ω extent of saturation of particle phase, with reference to initial and final concentrations

$*$ equilibrium

LITERATURE CITED

1. Acrivos, Andreas, and Theodore Vermeulen, cited in reference (41).
2. Anzelius, A., Z. angew. Math. Mech., 6, 291 (1926).
3. Baddour, R. F., and R. D. Hawthorn, Ind. Eng. Chem., 47, 2517 (1955).
4. Bauman, W. C., and J. Eichhorn, J. Am. Chem. Soc., 69, 2830 (1947).
5. Beaton, R. H., and C. C. Furnas, Ind. Eng. Chem., 33, 1500 (1941).
6. Bohart, G. S., and E. Q. Adams, J. Am. Chem. Soc., 42, 523 (1920).
7. Boyd, G. E., A. W. Adamson, and L. S. Myers, Jr., J. Am. Chem. Soc. 69, 2836, 2849 (1947).
8. Boyd, G. E., and B. A. Soldano, J. Am. Chem. Soc. 75, 6091, 6107 (1953); B. A. Soldano et al., Ibid., 77, 1331, 1339 (1955).
9. Carberry, J. J., and R. H. Bretton, A. I. Ch. E. Journal, 4, 367 (1958).
10. DeVault, Don, J. Am. Chem. Soc., 65, 532 (1943).
11. Donnan, F. G., Chem. Revs., 1, 73 (1924).
12. Drew, T. B., F. M. Spooner, and J. Douglas, cited in Klotz, I. M., Chem. Revs. 39, 241 (1946).
13. Ebach, E. A., and R. R. White, A. I. Ch. E. Journal, 4, 161 (1958).
14. Gilliland, E. R., and R. F. Baddour, Ind. Eng. Chem., 45, 330 (1953).
15. Gilliland, E. R., and D. R. Dewey II, U. S. Patent 2,741,591 (April 10, 1956).

16. Glueckauf, Eugen, Trans. Faraday Soc., 51, 34 (1955).

17. Glueckauf, Eugen, and J. I. Coates, J. Chem. Soc., 1947, 1315.

18. Gregor, H. P., J. Colloid Sci., 6, 20 (1951).

19. Hiester, N. K., R. K. Cohen, and R. C. Phillips, Chem. Eng. Progress Symposium Series, 50, no. 14, 63 (1954).

20. Hiester, N. K., R. K. Cohen, and R. C. Phillips, Ibid., 23 (1954).

21. Hiester, N. K., C. F. Fields, R. C. Phillips, and S. B. Radding, Chem. Eng. Progress, 50, 139 (1954).

22. Hiester, N. K., S. B. Radding, R. L. Nelson, Jr., and Theodore Vermeulen, A. I. Ch. E. Journal, 2, 404 (1956).

23. Hiester, N. K., and Theodore Vermeulen, Chem. Eng. Progress, 48, 505 (1952); J. Chem. Phys., 16, 1087 (1948).

24. Hougen, O. A., and W. R. Marshall, Chem. Eng. Progress, 43, 197 (1947).

25. Jacques, Gabriel, and Theodore Vermeulen, Univ. of Calif. Radiation Lab. Report 8029 (1957); A. I. Ch. E. Journal, paper submitted.

26. Koble, R. A., and T. E. Corrigan, Ind. Eng. Chem., 44. 383 (1952).

27. Lapidus, Leon, and N. R. Amundson, J. Phys. Chem., 56, 984 (1952).

28. Martin, A. J. P., and R. L. M. Synge, Biochem. J., 35, 1385 (1941).

29. Mayer, S. W., and E. R. Tompkins, J. Am. Chem. Soc., 69, 2866 (1947).

30. McHenry, K. W., and R. H. Wilhelm, A. I. Ch. E. Journal, 3, 83 (1957).

31. Michaels, A. S., Ind. Eng. Chem., 44, 1922 (1952).

32. Opler, Ascher, and N. K. Hiester, "Tables for Predicting the Performance of Fixed-Bed Ion Exchange", Stanford Research Institute, Menlo Park, California (1954).

33. Rice, S. T., and F. E. Harris, Z. physik. Chem., n.s., 8, 207 (1956); J. Chem. Phys. 24, 1258 (1956).

34. Selke, W. A., and Harding Bliss, Chem. Eng. Progress, 46, 509 (1950).

35. Sillén, L. G., and Erik Ekedahl, Arkiv. Kemi Mineral. Geol. A22, nos. 15 and 16 (1946).

36. Sips, R., J. Chem. Phys., 16, 490 (1948).

37. Strain, H. H., Anal. Chem., 23, 816 (1951).

38. Thomas, H. C., J. Am. Chem. Soc., 66, 1664 (1944); Ann. N. Y. Acad. Sci., 49, 161 (1948).

39. Van Deemter, J. J., F. J. Zuiderweg, and A. Klinkenberg, Chem. Eng. Sci., 5, 271 (1956).

40. Vasishth, R. C., and M. M. David, A. I. Ch. E. Journal, paper submitted.

41. Vermeulen, Theodore, in "Advances in Chemical Engineering", 2, 147-208, T. B. Drew and J. W. Hoopes, Jr., editors; New York: Academic Press (1958).

42. Vermeulen, Theodore, Ind. Eng. Chem., 45, 1664 (1953).

43. Vermeulen, Theodore, and N. K. Hiester, Chem. Eng. Progress Symposium Series, 55, no. 00, 000 (1959).

44. Vermeulen, Theodore, and N. K. Hiester, Ind. Eng. Chem., 44 636 (1952).

45. Vermeulen, Theodore, and N. K. Hiester, J. Chem. Phys., 22, 96 (1954).

46. Walter, J. E., J. Chem. Phys., 13, 229 (1945).

47. Weiss, J. E., J. Chem. Soc., 1943, 297.

48. Wicke, E., Kolloid-Z. 167, 289 (1939).

49. Wilson, J. N., J. Am. Chem. Soc., 62, 1583 (1940).

CAPTIONS FOR FIGURES

(1) Representative types of sorption equilibria.

(2) Sorption isotherms plotted on relative-concentration scales.

(3) Equilibrium for Fe^{+++} replacing H^+ on Dowex-50 resin (40), showing separation-factor fit ($r = 1/K = 0.125$).

(4) Effects of Peclet group, distribution ratio, and diffusivity ratio on H.T.U. ($= N/h$) or H.R.U. ($= N_R/h$).

(5) Effect of equilibrium parameter and N.T.U. on breakthrough history.

(6) Dimensionless breakthrough behavior at $r = 1$; the J function.

(7) Breakthrough curves for Fe^{+++} replacing H^+ on Dowex-50 columns.

(8) Typical elution curves, concentration vs. time, showing the influence of equilibrium parameter.

(9) Chromatogram for K^+ displaced by Na^+, using Dowex-50 resin (3).

(10) McCabe-Thiele diagram for separation of trace components with two theoretical contacts.

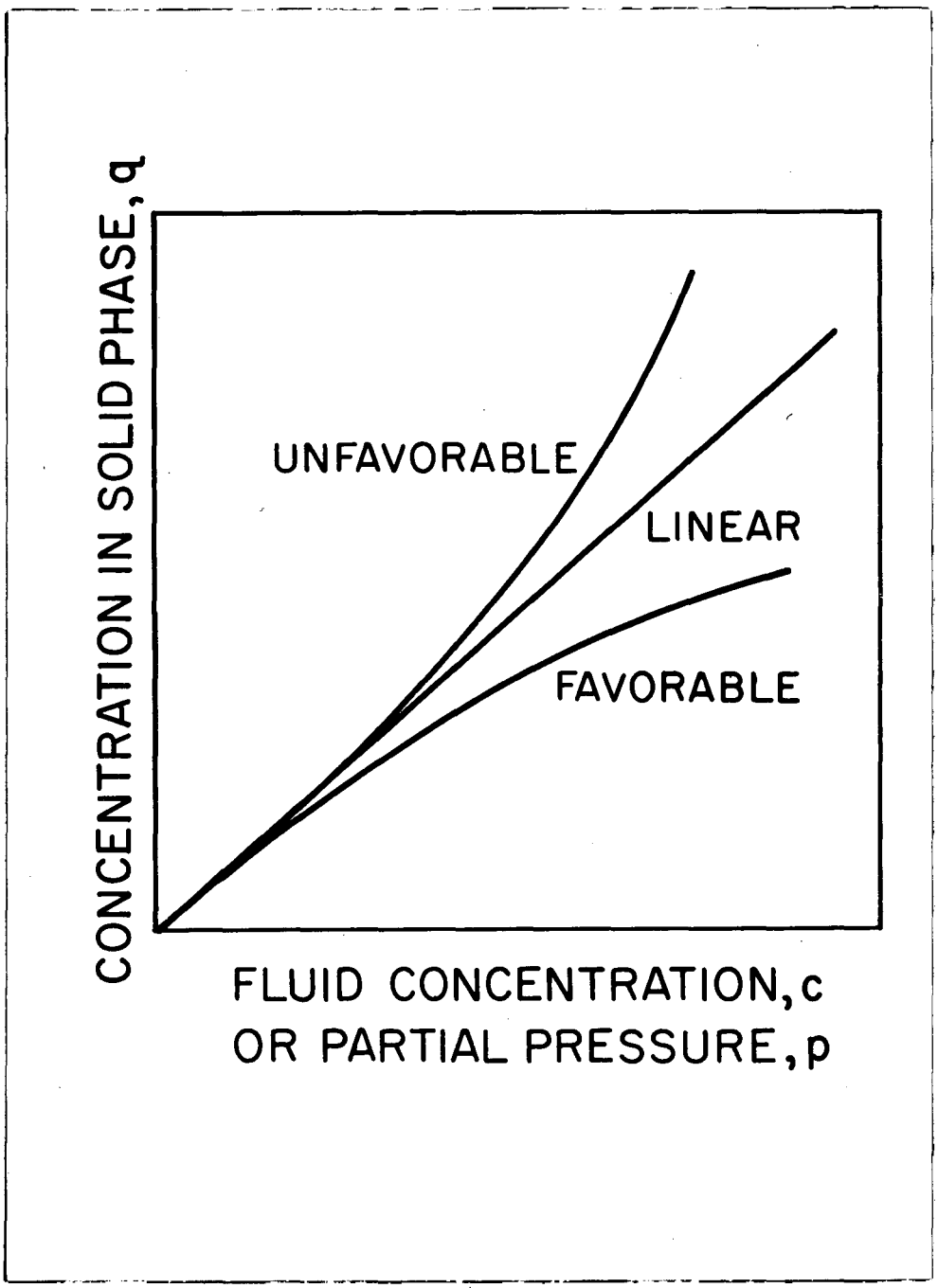
CONCENTRATION IN SOLID PHASE, q
UNFAVORABLE
LINEAR
FAVORABLE
FLUID CONCENTRATION, c
OR PARTIAL PRESSURE, p

Fig 1

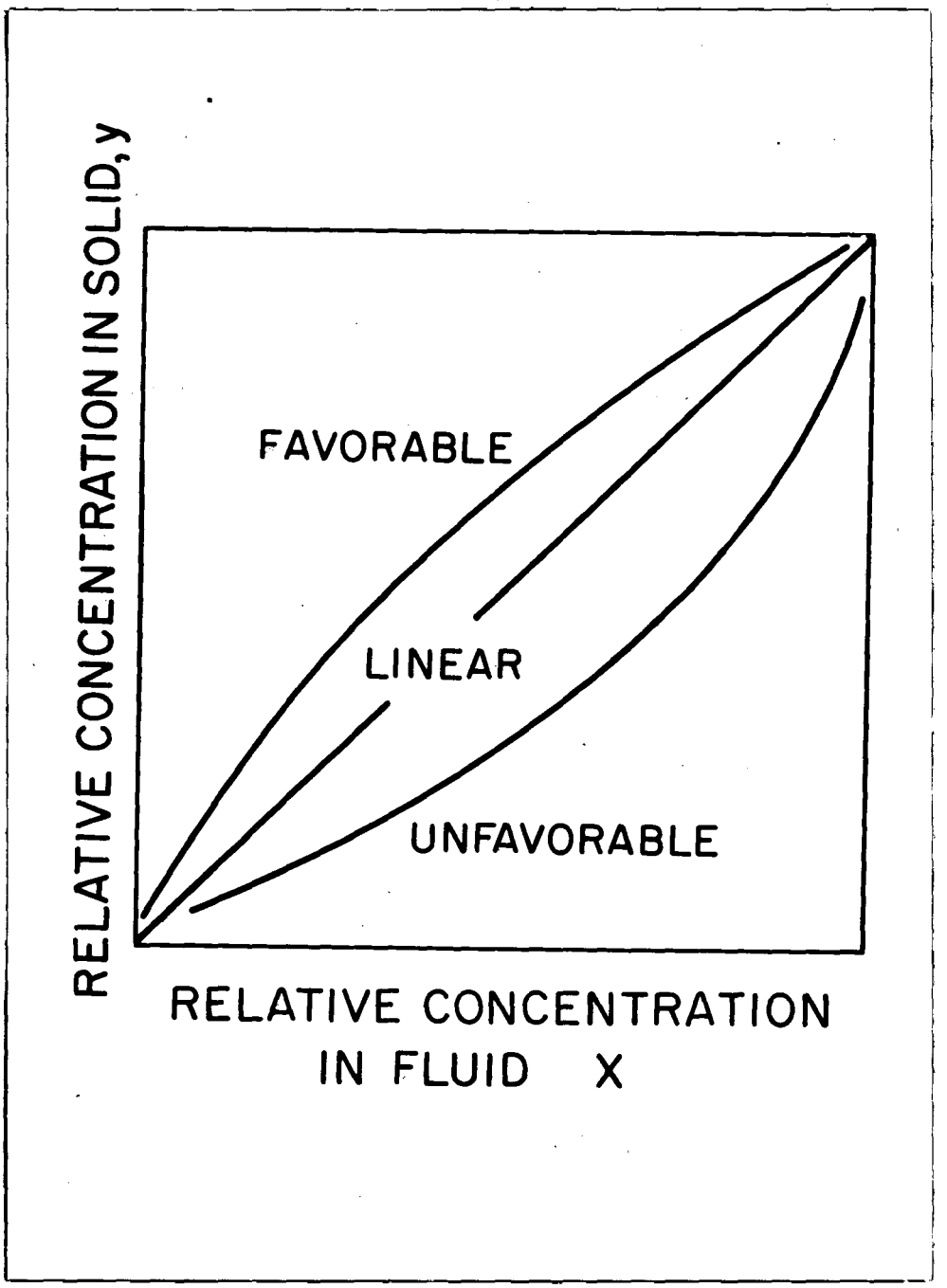
RELATIVE CONCENTRATION IN SOLID, y
FAVORABLE
LINEAR
UNFAVORABLE
RELATIVE CONCENTRATION
IN FLUID X

Fig 2

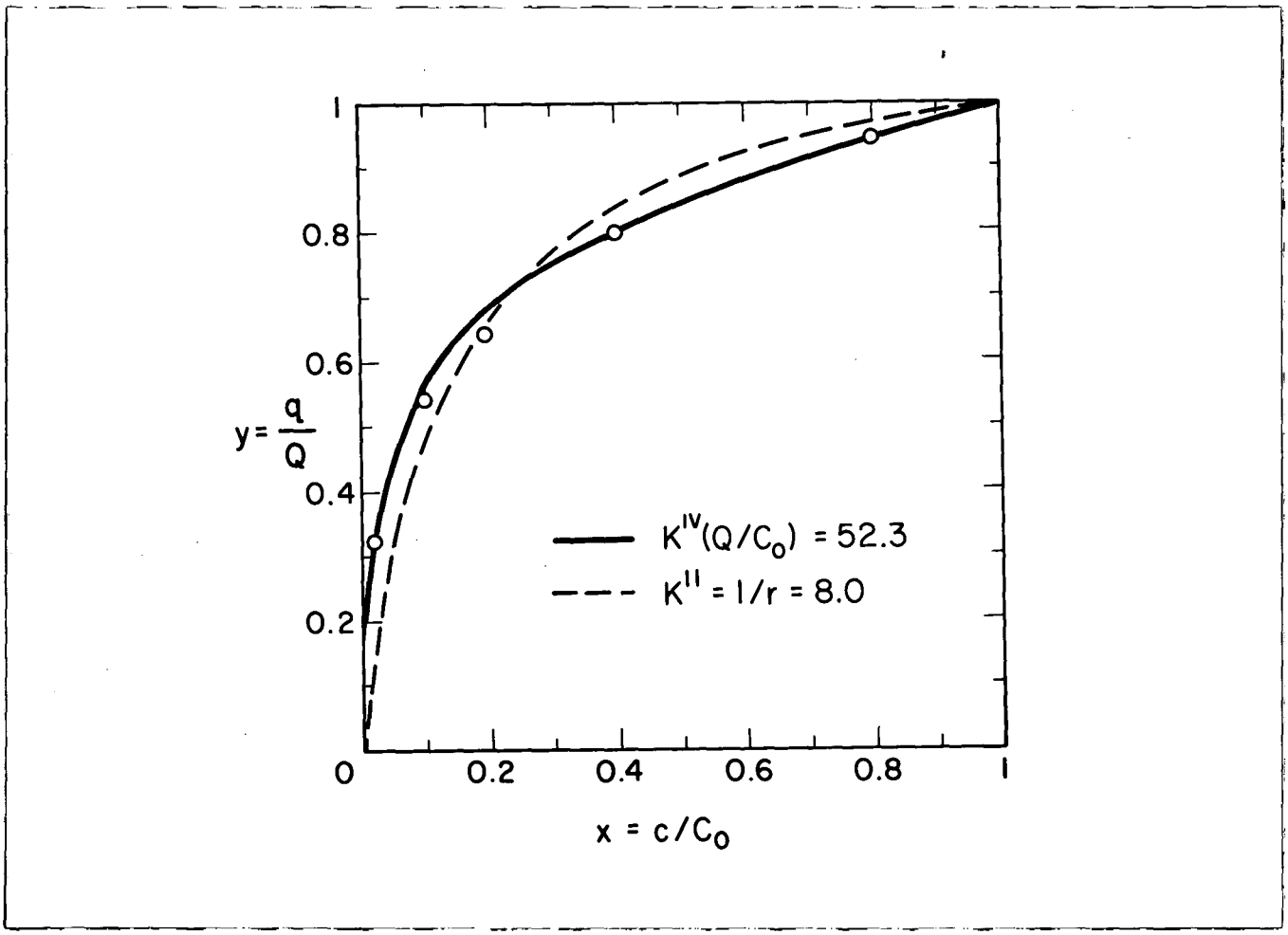

Fig. 3

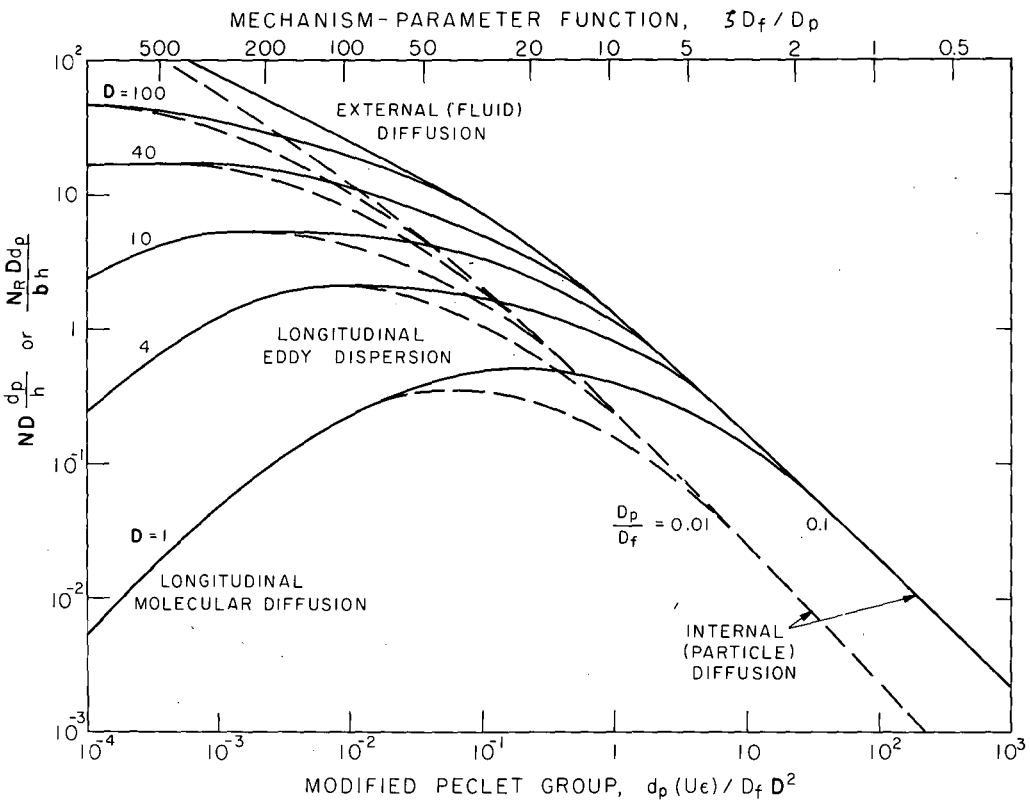
MECHANISM-PARAMETER FUNCTION, $\mathfrak{F} D_f / D_p$
500
200
100
50
20
10
5
2
1
0.5
10^2
D = 100
40
10
4
D = 1
EXTERNAL (FLUID) DIFFUSION
LONGITUDINAL EDDY DISPERSION
LONGITUDINAL MOLECULAR DIFFUSION
$\frac{D_p}{D_f}$ = 0.01
0.1
INTERNAL (PARTICLE) DIFFUSION
$ND\frac{d_p}{h}$ or $\frac{N_R D d_p}{b h}$
1
10^{-1}
10^{-2}
10^{-3}
10^{-4}
10^{-3}
10^{-2}
10^{-1}
1
10
10^2
10^3
MODIFIED PECLET GROUP, $d_p (U\epsilon) / D_f D^2$

Fig. 4

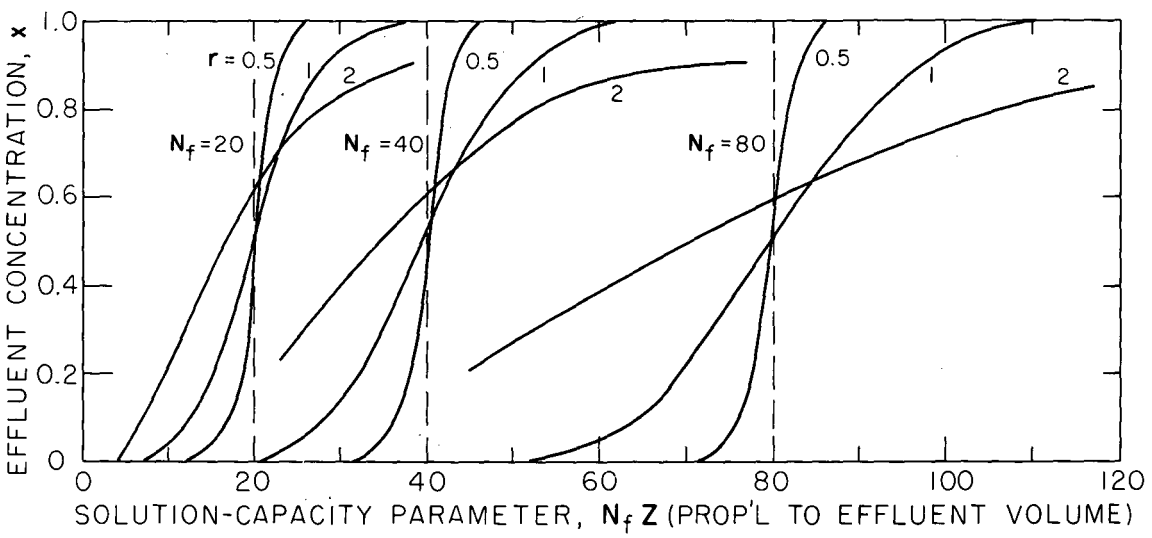

NOTE: r = 0.5 HAS CONSTANT PATTERN
r = 2 HAS PROPORTIONATE PATTERN

Fig. 5

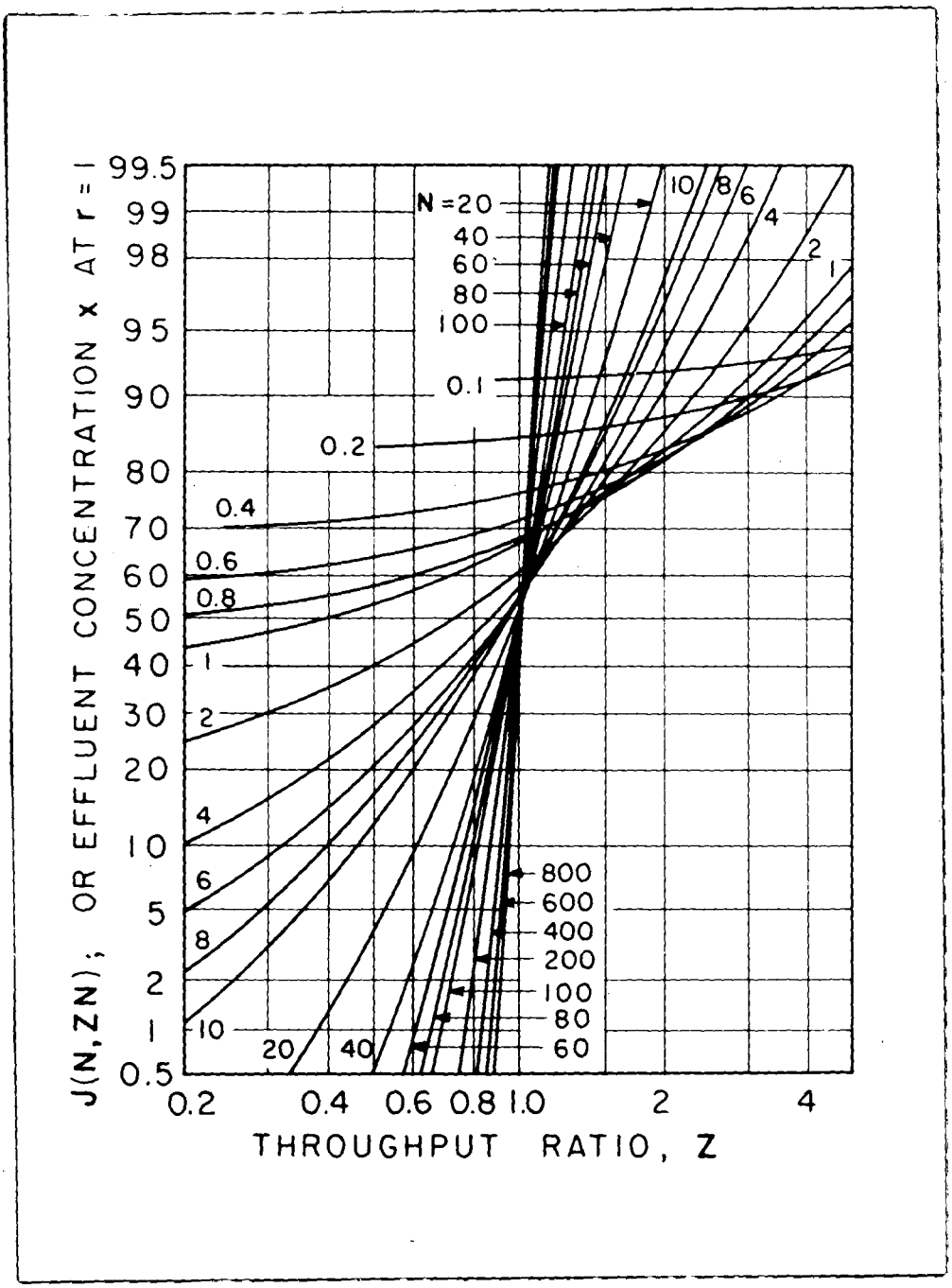
J(N,ZN); OR EFFLUENT CONCENTRATION x AT r = 1
99.5
99
98
95
90
80
70
60
50
40
30
20
10
5
2
1
0.5
N = 20
40
60
80
100
0.1
0.2
0.4
0.6
0.8
1
2
4
6
8
10
20
40
800
600
400
200
100
80
60
10
8
6
4
2
1
0.2
0.4
0.6
0.8
1.0
2
4
THROUGHPUT RATIO, Z

Fig. 6

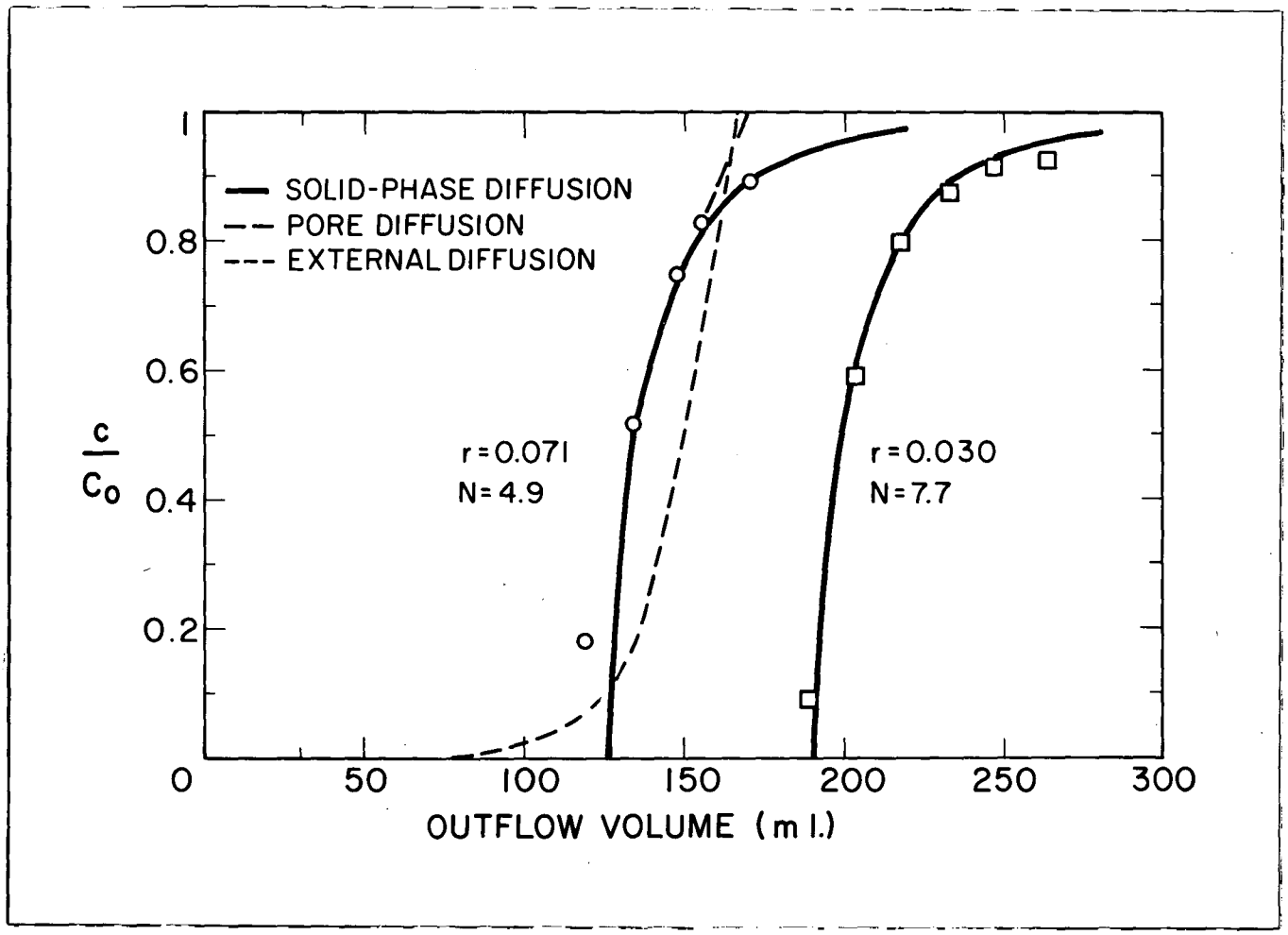
SOLID-PHASE DIFFUSION
PORE DIFFUSION
EXTERNAL DIFFUSION
r = 0.071
N = 4.9
r = 0.030
N = 7.7
c/Co
OUTFLOW VOLUME (ml.)
0
0.2
0.4
0.6
0.8
1
0
50
100
150
200
250
300

Fig. 7

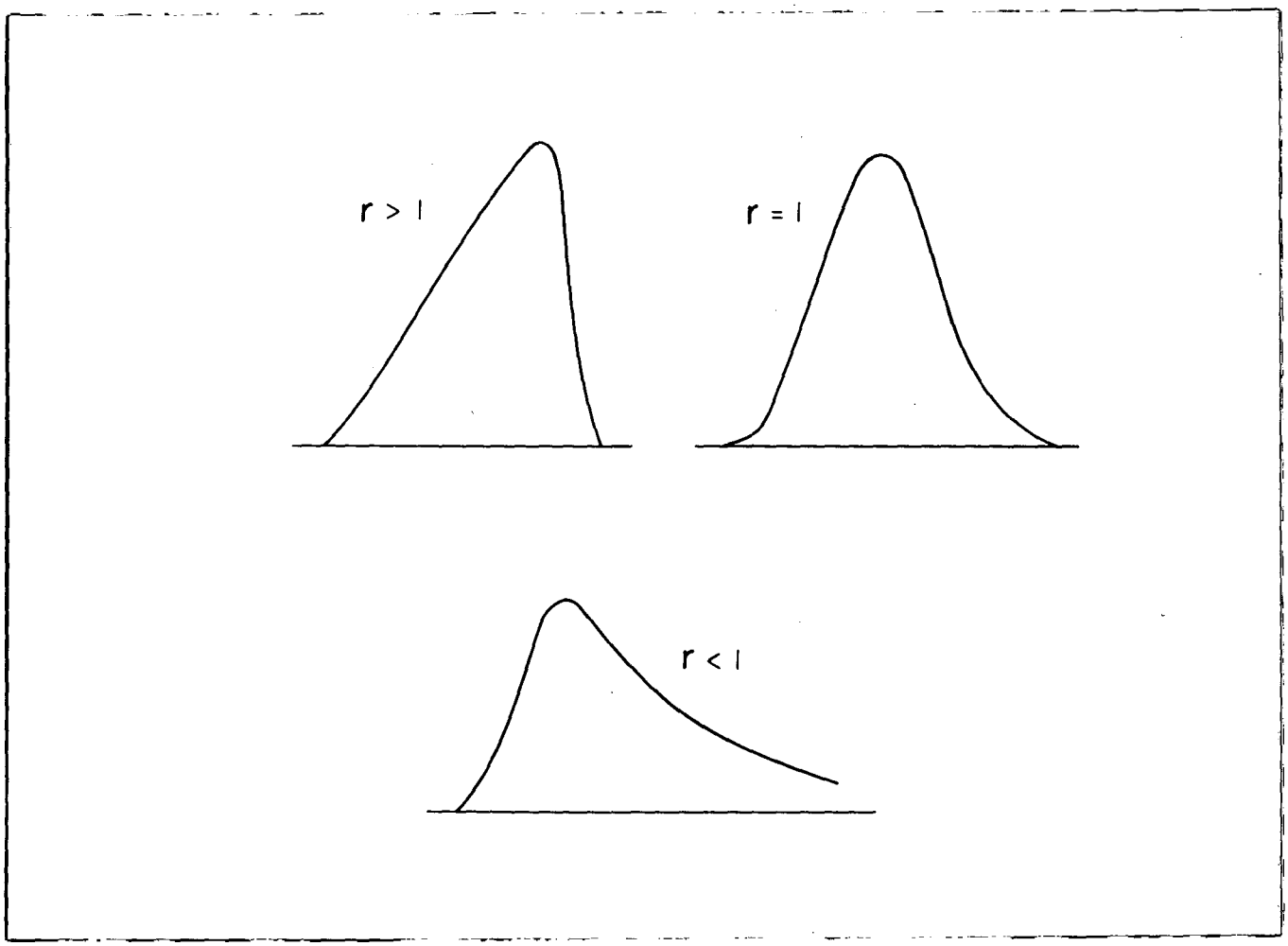

Fig. 8

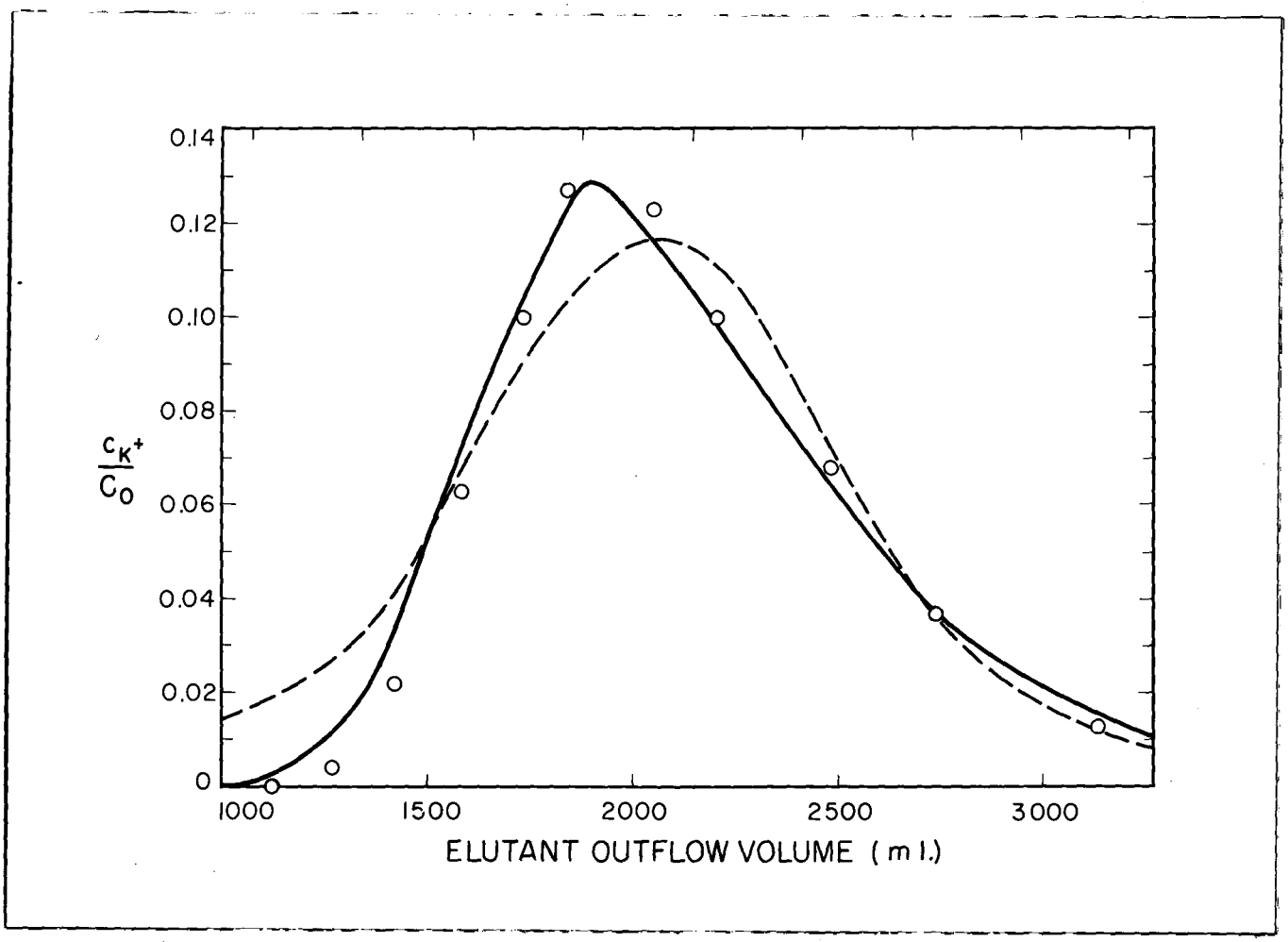
0.14
0.12
0.10
0.08
0.06
0.04
0.02
0
$\frac{C_{K^+}}{C_0}$
1000
1500
2000
2500
3000
ELUTANT OUTFLOW VOLUME (m l.)

Fig. 9

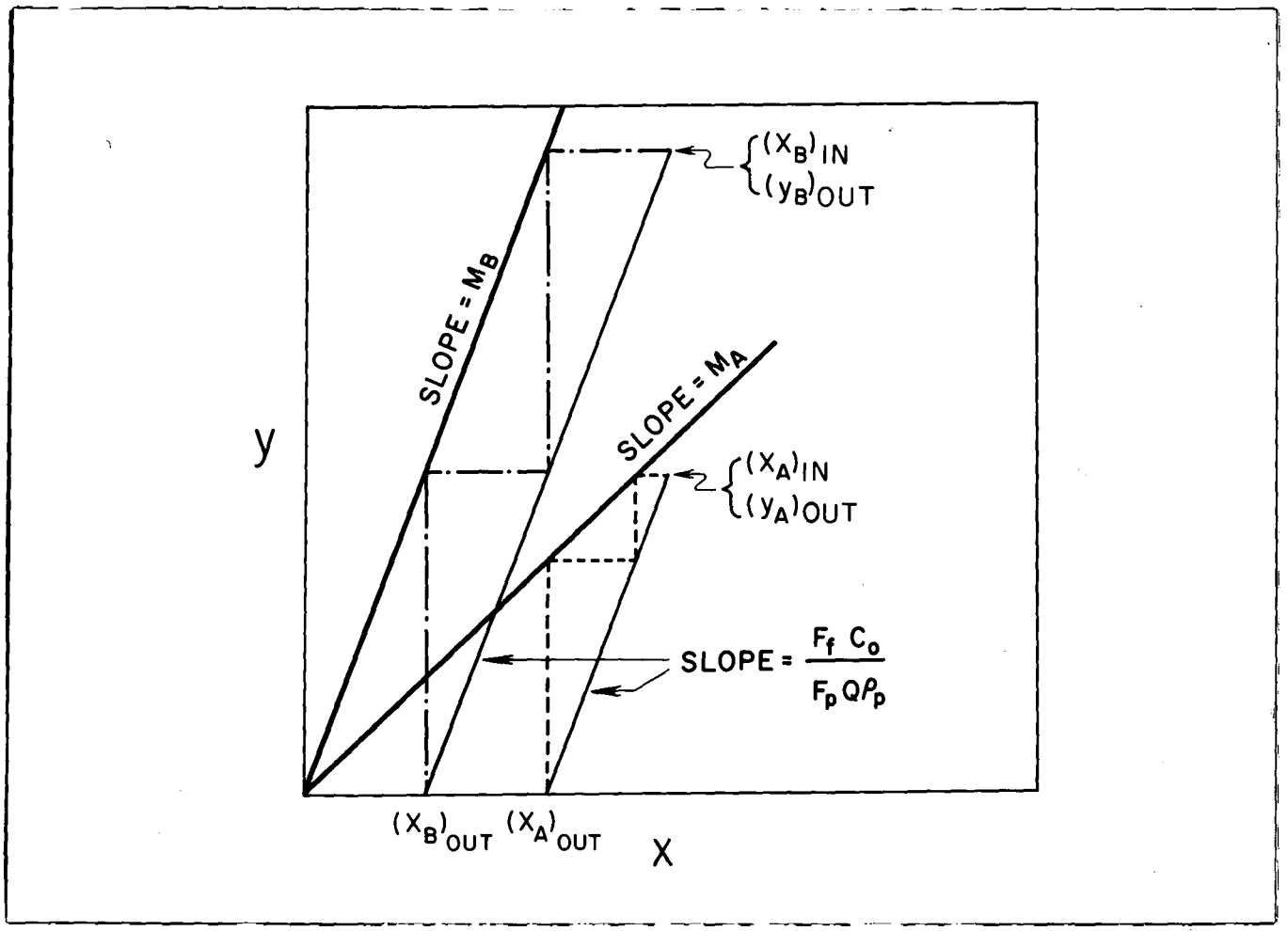
y
X
SLOPE = M_B
SLOPE = M_A
$(X_B)_{IN}$
$(y_B)_{OUT}$
$(X_A)_{IN}$
$(y_A)_{OUT}$
SLOPE = $\frac{F_f C_o}{F_p Q \rho_p}$
$(X_B)_{OUT}$
$(X_A)_{OUT}$

Fig. 10